Formation Response of High Frequency Electromagnetic Waves

Problem presented by

Khaled Hadj-Sassi and Patrice Ligneul

Schlumberger Carbonate Research Dhahran

Executive Summary

Core samples from rock formations respond to electromagnetic radiation based on an effective permittivity, which depends on the conductivity and permittivity of the constituent components of the rock, as well as the geometric structure of these constituents and the frequency of the radiation. This study analyzes the effect, for radiation of 1 to 100 Mhz, of discrete inclusions having a different permittivity from the surrounding medium. The focus is on the effect of certain geometric features, namely, the individual size of the inclusions, their overall volume fraction, the presence of sharp edges, and their aspect ratio.

It is found that the volume fraction has the strongest impact on the effective permittivity, linear at first but higher order at higher volume fractions. The aspect ratio of the inclusions has a moderate effect, which is exaggerated in the extreme case of needle-like inclusions, and which can also be seen in a stronger nonlinearity. There is also a possibility that some features in the shape of the inclusion boundaries may influence the frequency dependence of the effective permittivity. Inclusion size and sharp edges have negligible effect.

Version 1.0
July 13, 2011
iii+12 pages

Report coordinator

K. Hadj-Sassi and R. Clawson

Contributors

Daniel Binham (KAUST, Saudi Arabia)
Richard Clawson (KAUST, Saudi Arabia)
Nick Hale (OCCAM, UK)
John Hinch (Cambridge University, UK)
John Ockendon (University of Oxford, UK)
Braxton Osting (Columbia University, USA)
Zaid Sawlan (KAUST, Saudi Arabia)
Jens Schneider (KAUST, Saudi Arabia)
Chengcheng Tang (KAUST, Saudi Arabia)

KSG 2011 was organised by
King Abdullah University of Science and Technology (KAUST)
In collaboration with
Oxford Centre for Collaborative Applied Mathematics (OCCAM)

Contents

1 Introduction

The proposed problems aim to enhance our understanding of the relationship between the polarized high frequency electromagnetic wave and the texture of the rock. The texture means here the size and the shape of pores and particles dispersed in the heterogeneous medium. These inclusions may have spherical, elliptical and/or rhombic shapes; and may be represented by different size scales. The interaction of the inclusions that may generate a secondary effect on the polarization outside the inclusion will be investigated as well. The frequency range of interest here is from 1 to 100 MHz.

Therefore, the purpose of the problems that we will be discussing in the Study Group is to understand how the high frequency EM waves behave with respect to the rhombic shape with sharp edges and the needle effect of very long, narrow inclusions, and also to determine if there is any inclusion size effect and any secondary effect due to the coupling of polarization between inclusions.

2 Background

2.1 Maxwell's Equations

Maxwell's equations to describe the EM phenomenon are expressed in differential form in Equation (1). The first equation represents Faraday's law. The second equation is Ampere's law where we see the introduction of the displacement current. The third and fourth equations represent Gauss' law for the electric and magnetic fields where the divergence of the electric displacement is equal to the charge density ρ_e, and the divergence of the magnetic flux is zero.

$$\begin{aligned} \nabla \times \boldsymbol{E}(\boldsymbol{r},t) &= -\frac{\partial \boldsymbol{B}(\boldsymbol{r},t)}{\partial t} \\ \nabla \times \boldsymbol{H}(\boldsymbol{r},t) &= \boldsymbol{J}(\boldsymbol{r},t) + \frac{\partial \boldsymbol{D}(\boldsymbol{r},t)}{\partial t} \\ \nabla \cdot \boldsymbol{D}(\boldsymbol{r},t) &= \rho_e(\boldsymbol{r}) \\ \nabla \cdot \boldsymbol{B}(\boldsymbol{r},t) &= 0 \end{aligned} \tag{1}$$

2.2 Constitutive Equations

The electric displacement and the magnetic induction $\boldsymbol{D}$ and $\boldsymbol{B}$ are related to the field intensities $\boldsymbol{E}$ and $\boldsymbol{H}$ via constitutive relations, where the form depends on the material in which the fields exist. In these constitutive relations, we assume that the medium is homogeneous and isotropic. $\hat{\epsilon}_r$ and μ_r are respectively the permittivity and the permeability of the formation.

$$\begin{aligned} \boldsymbol{D}(\boldsymbol{r},t) &= \epsilon_0 \hat{\epsilon}_r(\boldsymbol{r},t)\boldsymbol{E}(\boldsymbol{r},t) \\ \boldsymbol{B}(\boldsymbol{r},t) &= \mu_0 \mu_r \boldsymbol{H}(\boldsymbol{r},t) \\ \boldsymbol{J}(\boldsymbol{r},t) &= \hat{\sigma}(\boldsymbol{r},t)\boldsymbol{E}(\boldsymbol{r},t) \end{aligned} \tag{2}$$

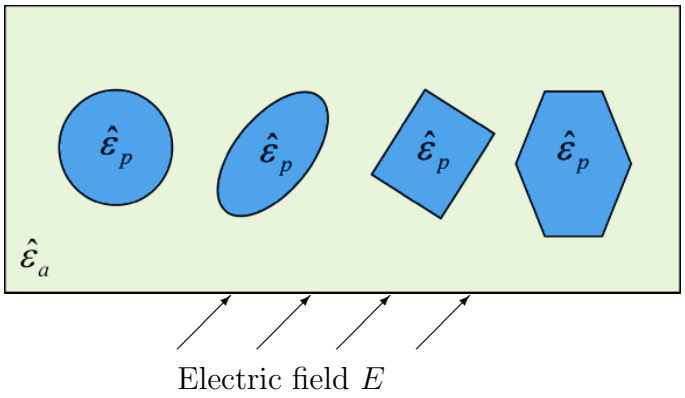

Figure 1: Two phase system with four inclusion shapes of complex permittivity $\hat{\epsilon}_p$ dispersed in the background medium of complex permittivity $\hat{\epsilon}_a$.

The third equation represents here, Ohm's law to express the relationship between the electric current and the electric field through the conductivity property $\hat{\sigma}$ of the formation.

The constitutive equations of Equation (2) are defined in an homogeneous and isotropic medium. However, in the inhomogeneous and anisotropic formation, there is another term to be added to represent the induced polarization of the formation as we can see in Equation (3) below.

$$\boldsymbol{D}(\boldsymbol{r},t) = \epsilon_0 \hat{\epsilon}_a(\boldsymbol{r},t)\boldsymbol{E}(\boldsymbol{r},t) + P(\hat{\epsilon}_p) \tag{3}$$

In other words, the presence of the inclusion with different material properties from the background medium generates a new polarization term for the induced electric field. This polarization is a function of the inclusion's shape as well as its material type. The size may also have an effect.

At the frequencies of intrest (1 to 100 Mhz), the wavelength is much longer than size of typical inclusions, in the sequel we treat the external field as uniform. We also treat it as static, except for a brief discussion of response times in Section 3.1.

3 Study Group Results

3.1 Inclusion size effect on the polarized high frequency EM wave

In this section, we will investigate the effect of inclusion size on the polarized electric field. Through the Study Group discussion, we concluded that the size of the isolated inclusions may not have an effect on the polarizability of the overall medium. Rather, the total volume fraction of the inclusions represents the dominant effect. More details are provided in the sections below.

Conducting (brine-filled) cavity in a uniform external field

The brine contains a free charge density ρ of positive ions, and likewise for negative ions, see Figure 2. When a uniform external field is applied, the positive ions shift with the field, until a layer of some thickness x_0 has accumulated at the boundary to form a surface charge density ρ_s. Negative ions shift likewise to the opposite side (not shown).

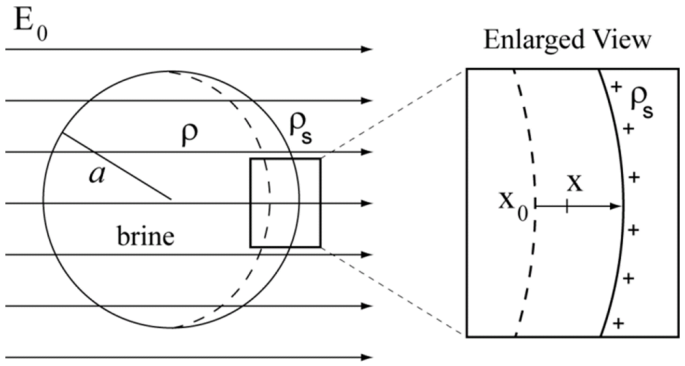

Figure 2: Conducting cavity in uniform external field

Static case

Solution of Laplace's equation gives the electric potential as well as the surface charge density. For a spherical cavity of radius a, this is

$$\rho_s = 3\epsilon_0 E_0 \cos\theta. \tag{4}$$

This is *independent* of the cavity radius, so the total surface charge q on the positive side is simply proportional to the surface area. The dipole moment d of the cavity is proportional to the product of q with the separation between the positive and negative sides, which is proportional to a. This leads to the dipole moment d being proportional to the volume V,

$$d \propto qa \propto a^3 \propto V. \tag{5}$$

For the sphere, it can be shown that the constant of proportionality is $3\epsilon_0 E_0$. For other geometries this will vary, but the dependence on (surface charge) $\times$ (charge separation) will persist, so the dipole will always be proportional to ℓ^3, where ℓ is some characteristic length of the cavity. That is, the dipole moment will always be proportional to the cavity volume (unless the shape produces some extreme relationship between surface area and volume).

For a collection of such cavities in a solid, the total dipole moment produced will be the sum of the individuals (if they are sparse enough to have negligible interaction), so the dipole moment density will be proportional to the amount of cavity volume per unit total volume, i.e., the volume fraction of cavities.

The total induced dipole moment density depends on the external electric field, but if we factor that out we get the polarizability, which determines the electric permittivity ϵ of the medium. The cavities therefore contribute to ϵ, and their contribution depends on their volume fraction, but not on their individual size, and only weakly on their shape.

Time/frequency dependence

When an external field is applied and the ions begin to shift, it takes some time for the surface charge to build up and bring the system to a new equilibrium. We refer to this as the relaxation time.

An estimate of this relaxation time is calculated (See Appendix A for details), and we find that the charges drift toward their new equilibrium positions at a rate that decays exponentially,

$$x = x_0 e^{-t/\tau}, \tag{6}$$

with relaxation time

$$\tau = \gamma \frac{\epsilon_0}{\mu \rho}, \tag{7}$$

where ρ is the ionic charge density in the brine, μ is the ionic mobility, and γ is a dimensionless factor related to how the geometry of the shape influences the final (equilibrium) surface charge density. For shapes that do not have extreme geometries, $\gamma \sim 1$. Putting in some typical numbers we find $\tau \sim 10^{-9}$s, just about on the order of the period of the highest frequency waves of interest in this study. (Note, though, that these figures are quite rough, and a factor of 10 or more might easily show up in a more accurate calculation). This means that we may be able to expect a significant drop in the effective permittivity toward the higher end of our range, but it will depend only on the volume fraction.

The one thing we might hope for is that the relaxation dynamics could be affected by complicated structure in the cavity boundaries, which might significantly change the value of the geometric factor γ. Specifically, the approach to equilibrium is not uniform, but position dependent, and γ should actually have position dependence, being affected by the charge density in the surface nearby. Therefore, in areas with for example sharp corners or heavy reticulation, γ may be larger, and this could increase the average (effective) τ for the whole cavity. This would in turn reduce the frequency at which the permittivity begins to drop. More calculation is required to explore this.

3.2 Secondary Effect: Interaction effect between inclusions

The secondary effect was demonstrated numerically. Figure 3 shows the effective permittivity of the medium in which we insert different inclusion shapes. Each cell/domain containing an inclusion type is surrounded by similar cells, so that a periodic medium is formed. As can be seen, the effective permittivity response curves depend linearly on the volume fraction of the inclusion (volume fraction =

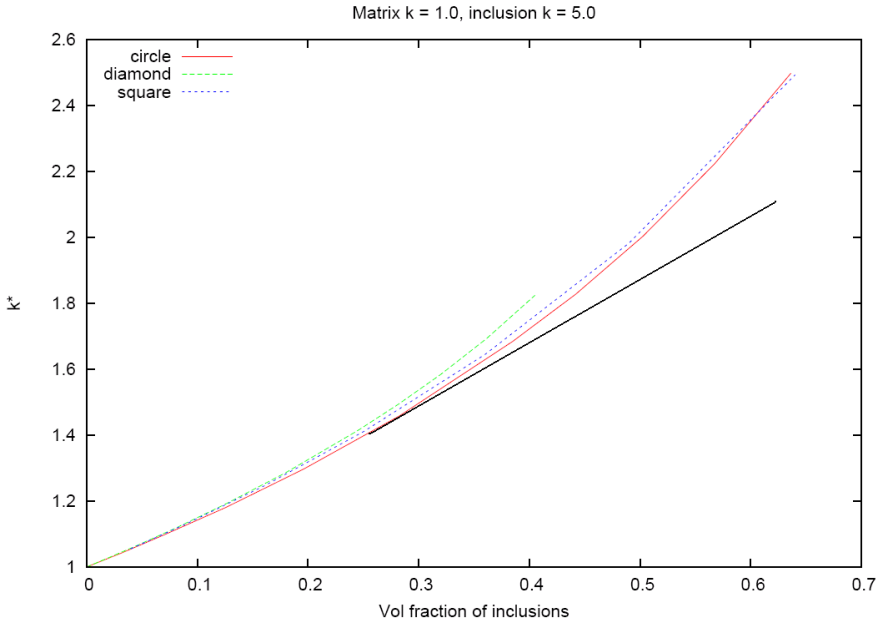

Figure 3: The secondary effect due to the interaction between inclusions is represented by the curvature of the effective permittivity responses.

volume of inclusion / volume of periodic cell). However the curves are not strictly linear, for as the inclusions fill more and more of their cells, the distortion each induces in the external field begins to overlap with inclusions in neighboring cells. The tangent of the curves (in black color) represents the response of the isolated inclusion. The curvature seen in the plotted responses indicates the effect of the interaction between inclusions, the so called secondary effect.

3.3 Sharp Edge Effect of Rhombic Inclusion

The purpose of this proposed problem is to investigate the effect of an inclusion with sharp edges, such as a rhombic shape, and to characterize the needle effect.

Numerical simulations have been performed to investigate this problem using the finite difference method. The electric potential field, in a periodic medium, satisfies the equation: $\nabla \cdot [\epsilon(x)\nabla\phi] = 0$. We only consider the real part of complex permittivity in this study. The background domain has a real permittivity $\hat{\epsilon}_1$. The inclusion is represented by a higher permittivity $\hat{\epsilon}_2$. The map of the potential field calculated in a periodic cell with a square shape inclusion is shown in Figure 4.

The effective permittivity of the system is computed and plotted versus the volume fraction (volume fraction = volume of inclusion / volume of periodic cell). The results of effective permittivity of the medium versus the volume fraction for the circle, square, diamond and ellipsoidal inclusions are displayed in Figure 5.

As shown, the effective permittivity linearly depends on the volume fraction of the inclusion. In addition, at a given volume fraction, the effective permittivities have almost the same response for the circle and the inclusions with sharp edges such as the diamond and square. This means that there is no sharp edge effect and

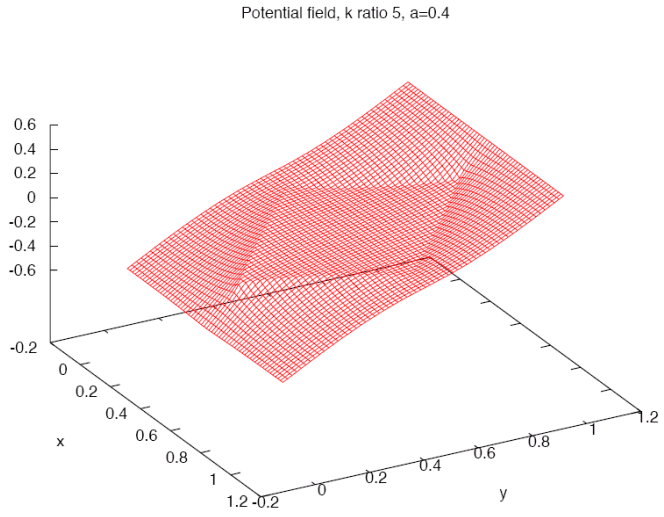

Figure 4: The computed potential field in a periodic cell with a square inclusion

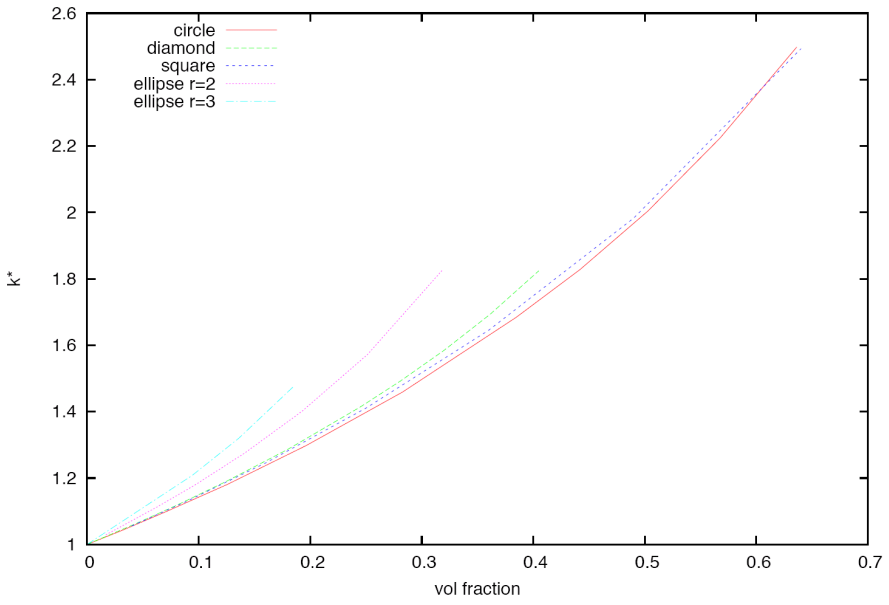

Figure 5: Comparison of the effective permittivity responses of periodic cells with different inclusion shapes. The effective permittivity of the background and the inclusion are, respectively, $\epsilon_1 = 1$ and $\epsilon_2 = 5$. Four inclusion shapes have been selected: circle, diamond, square and ellipsoids (with two aspect ratios r).

the singularity effect is neutralized in the polarization from such shapes. However, there is clearly an effect due to the aspect ratio of ellipsoidal inclusions, compared with sharp edge and circle inclusions. A higher aspect ratio generates a higher permittivity for a given volume fraction, as well as stronger second order effects.

3.4 Needle Effect: Slender Body Theory

In this section, the effective permittivity of a cell domain with an extremely elongated ellipsoid, which may exhibit a needle effect, will be expressed analytically. The slender body theory will be applied to express the electric potential and the polarization outside the inclusion. The transverse polarization outside the inclusion is neglected here and we only focus on the longitudinal one. A schematic representation of the ellipsoidal inclusion is shown in Figure 6 (the actual aspect ratio would be much greater). We show below the results for the electric potential and the effective permittivity in this section. (See Appendix B for details.)

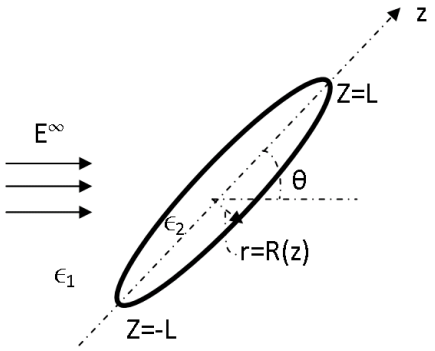

Figure 6: Elongated ellipsoid of permittivity ϵ_2

The electric potential outside the inclusion is:

$$\phi = E^{\infty} z \cos\theta - \frac{1}{4\pi\epsilon_1} \int_{-L}^{L} \frac{q(z')dz'}{\sqrt{r^2 + (z-z')^2}} \tag{8}$$

In the case of an ellipsoidal inclusion it can be shown that the potential inside the inclusion is linear and axial, given by:

$$\phi(z) = Ez \tag{9}$$

where E is a uniform electric field.

After the coupled inside-outside problem is solved, the resulting effective permittivity for a composite with a number density n of inclusions orientated randomly is expressed by

$$\epsilon^* = \epsilon_1 \left[1 + \frac{4\pi}{9} n L^3 \frac{\alpha^2}{\frac{\epsilon_1}{\epsilon_2} + \left(\ln \frac{1}{\alpha} + O(1) \right) \alpha^2} \right] \tag{10}$$

where L is the length of the ellipse's long semi-axis, and α is the aspect ratio.

While this was derived for an isolated slender body requiring $nL^3 \ll 1$ (fibers separated by more than L), the formula can be used for $nL^3 = O(1)$ by replacing $\ln \frac{1}{\alpha}$ by $\ln \frac{\text{fiber separation}}{\text{fiber diameter}}$.

3.5 Effective Medium/Homogenization Theory

A homogenization study has been done for a periodic medium. An analytical expression of the periodic medium ϵ_1 with an inclusion ϵ_2 has been formulated in 1D. In 2D, a computational solution is required for most inclusion shapes.

4 Conclusion

It has been found that the volume fraction has the strongest impact on the effective permittivity, linear at first but higher order at higher volume fractions. The aspect ratio of the inclusions has a moderate effect, which is exaggerated in the extreme case of needle-like inclusions, and which can also be seen in a stronger nonlinearity. There is also a possibility that some features in the shape of the inclusion boundaries may influence the frequency dependence of the effective permittivity. Inclusion size and sharp edges have negligible effect.

Bibliography

[1] Asami, K., Characterization of heterogeneous systems by dielectric spectroscopy, Prog. Polym. Sci. 27 (2002) 1617–1659.

[2] Babych, N., Kamotski, I., and Smyshlyaev, V., Homogenization of spectral problems in bounded domains with doubly high contrasts, Networks and Heterogeneous Media, 3 (2008) 413–436.

[3] Bensoussan, A., cLions , J-L., Papanic-Olaou, G., Asymptotic Analysis for Periodic Structures, Elsevier, Amsterdam, 1978

[4] Chen H.-S., and Acrivos A., On the Effective Thermal Conductivity of Dilute Slender Inclusions Suspensions Containing Highly Conducting, Proc. R. Soc. Lond. A 1976 349, 261–276.

[5] Fouque J.-P., Garnier J., Papanicolaou G. and Solna K., Wave Propagation and Time Reversal in Randomly Layered Media, Springer, 2007.

[6] Hinch E. J., Sherwood J. D., Chew W.C., and Sen P. N., Dielectric Response of a Dilute Suspension of Spheres with Thin Double Layers in an Asymmetric Electrolyte, J. Chem. SOC., Faraday Trans. 2, 1984,80,535–551

[7] Howell P, Kozyreff G, and Ockendon J., Applied Solid Mechanics, (Cambridge Texts in Applied Mathematics). Edition 2009.

[8] Jackson J. D., Classical Electrodynamics, Third Edition, 1998.

[9] Plawskey, J., Transport Phenomena Fundamentals, 2nd ed., CRC Press, Boca Raton, USA, 2010.

[10] Pride, S., Governing equations for the coupled electromagnetics and acoustics of porous media, Phys. Rev. B 50 (1994) 15,678–15,696.

[11] Smyshlyaev, V., Propagation and localization of elastic waves in highly anisotropic periodic composites via two-scale homogenization, Mechanics of Materials 41 (2009) 434–447.

Appendices

A Relaxation time for brine-filled cavity in uniform field

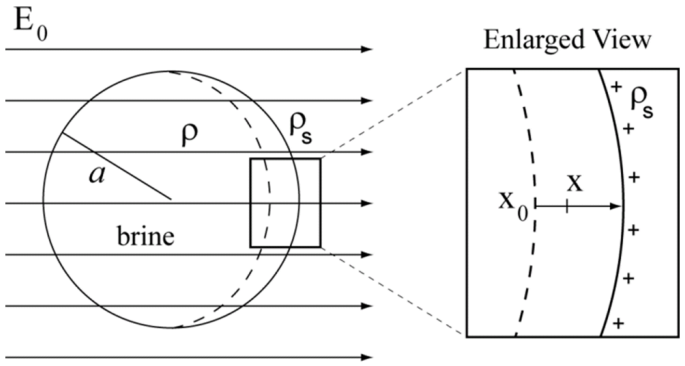

The inner boundary of the accumulation layer is represented by x in Figure A, with initial distance x_0. Under the influence of an electric field E it will move with the speed of the ions,

$$\dot{x} = -\mu E, \qquad x(0) = x_0, \tag{11}$$

where μ is the ionic mobility, a factor which determines the drift speed of the ions in the field. All quantities here are scalar magnitudes, and the negative sign is because x is decreasing as it approaches the cavity boundary. (Remark: we believe that when E changes, the drift speed follows it with no significant delay, so we ignore the time it takes to accelerate.)

Now E is the sum of the external field E_0, which we take to be a step function, and the induced polarization field E_p inside the cavity, $E(t) = E_0 + E_p(t), t > 0$. Furthermore, E_p is proportional to the amount of surface charge accumulated on the boundary. If the external field is applied as a step function, then E_p starts

at zero and reaches its maximum when the surface charge ρ_s has reached its final (equilibrium) value ρ_{sf}, at which point E_p must be equal and opposite E_0,

$$E_p(t) = -\frac{\rho_s(t)}{\rho_{sf}} E_0 \quad \Longrightarrow \quad E(t) = E_0 \left(1 - \frac{\rho_s(t)}{\rho_{sf}}\right). \tag{12}$$

The surface charge density is simply equal to the interior volume charge density times the amount of thickness that has already accumulated, $\rho_s(t) = \rho[x_0 - x(t)]$, but ρx_0 just represents the surface charge density after the whole accumulation layer has accumulated, which is ρ_{sf}. (Remark: there should actually be an angular factor in the expression for $\rho_s(t)$, but we'll ignore that for simplicity). Therefore, $\rho_s(t) = \rho_{sf} - \rho x(t)$, so that

$$E(t) = E_0 \frac{\rho}{\rho_{sf}} x(t). \tag{13}$$

Substituting this back into the equation for $\dot{x}$ we find

$$\dot{x} = -\mu E_0 \frac{\rho}{\rho_{sf}} x, \tag{14}$$

with solution

$$x = x_0 e^{-t/\tau}, \qquad \tau = \frac{\rho_{sf}}{\mu E_0 \rho}. \tag{15}$$

For a sphere we have $\rho_{sf} = 3\epsilon_0 E_0 cos\theta$. More generally, it will be $\gamma\epsilon_0 E_0$, where γ is some dimensionless proportionality factor of order unity that depends on the specific geometry. Thus, for simple shapes,

$$\tau = \gamma \frac{\epsilon_0}{\mu\rho}, \qquad \gamma \sim 1. \tag{16}$$

This depends only on the geometry and the ionic charge density and mobility, so the relaxation time will not be influenced by cavity size.

If the salt concentration is 50kppm, in water having 3.3×10^{22} mlc/cm^3, then the charge density for doubly ionized ions is

$$\rho = \frac{5 \times 10^4}{10^6} \times 3.3 \times 10^{22} \frac{\text{mlc}}{\text{cm}^3} \times 2 \times 1.6 \times 10^{-19} \frac{\text{C}}{\text{mlc}} = 5.2 \times 10^2 \frac{\text{C}}{\text{cm}^3}. \tag{17}$$

A rough value for the ionic mobility of doubly ionized sodium ions in water is (Plawsky 2010, p. 111)

$$\mu = 2 \times 5 \times 10^{-4} \frac{\text{cm}^2}{\text{V-s}}. \tag{18}$$

With $\epsilon_0 \approx 10^{-9} \frac{\text{C}}{\text{V-cm}}$, this leads to

$$\tau \approx \frac{10^{-9} \frac{\text{C}}{\text{V-cm}}}{5 \times 10^{-4} \frac{\text{cm}^2}{\text{V-s}} \times 5 \times 10^2 \frac{\text{C}}{\text{cm}^3}} = 4 \times 10^{-9} s. \tag{19}$$

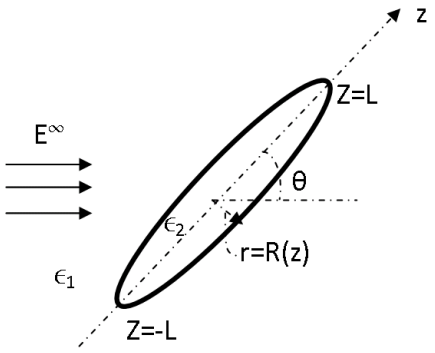

Figure 7: Slender body of permittivity ϵ_2

B Needle effect – Slender body theory

In this section, we describe the slender body theory to calculate the effective permittivity of a medium

The applied field is not perpendicular to the axis. The electric potential satisfies $\nabla \cdot [\epsilon(\boldsymbol{x})\nabla\phi] = 0$ and $\phi \xrightarrow{r\to\infty} \boldsymbol{E}^\infty \cdot \boldsymbol{x}$ assuming that the field is not perpendicular to the axis.

Integral representation of potential outside the inclusion:

$$\phi = \boldsymbol{E}^\infty \cdot \boldsymbol{x} - \int_{-L}^{L} \frac{q(z')dz'}{4\pi\epsilon_1\sqrt{r^2 + (z-z')^2}} \tag{20}$$

Evaluate ϕ on boundary, $\phi(R(z), z)$. Singular integral, logarithmic case where main contribution comes from $R << |z - z'| << L$,

$$\phi(R(z), z) = E^\infty \cos(\theta) z - \frac{1}{2\pi\epsilon_1} q(z) \left[\ln \frac{L}{R} + O(1)\right] \tag{21}$$

Inside body have axial field:

$$\epsilon_2 \frac{d\phi}{dz} \tag{22}$$

The flux inside the ellipsoid is:

$$Q(z) = \pi R^2(z)\epsilon_2 \frac{d\phi}{dz} \tag{23}$$

Divergence of flux inside equals flux/source into outside

$$q - \epsilon_1 \frac{d\phi}{dz}\frac{dR}{dz} 2\pi R = -\frac{dQ}{dz} \tag{24}$$

Hence coupled inside-outside problem

$$\phi(z) = E^\infty \cos(\theta) z - \frac{\ln \frac{L}{R} + O(1)}{2\pi\epsilon_1} \left[\epsilon_1 \frac{d\phi}{dz}\frac{d}{dz}(\pi R^2) - \frac{d}{dz}\left(\pi R^2 \epsilon_2 \frac{d\phi}{dz}\right)\right] \tag{25}$$

[N.B. case $\epsilon_1 = \epsilon_2$ has solution $\phi(z) = E^\infty \cos(\theta) z, q = 0$]

Now interested in case with $|\epsilon_2| \gg |\epsilon_1|$, (mod sign because might be complex)

$$\phi(z) = E^\infty \cos(\theta) z + \frac{\ln \frac{L}{R} + O(1)}{2} \frac{\epsilon_2}{\epsilon_1} \frac{d}{dz} \left(R^2 \frac{d\phi}{dz} \right) \tag{26}$$

See ϵ_2 has very little effect unless very big,

$$\epsilon_2 = O\left(\frac{\epsilon_1 \frac{L^2}{R^2}}{\ln \frac{L}{R}} \right) \tag{27}$$

The case of an ellipse is simple to solve

$$\frac{R^2}{b^2} + \frac{z^2}{L^2} = 1, \quad \text{i.e.,} \quad R^2(z) = b^2 \left(1 - \frac{z^2}{L^2} \right) \tag{28}$$

because clearly satisfied by uniform internal field E

$$\phi = Ez, \tag{29}$$

$$Ez = E^\infty \cos(\theta) z + \frac{\ln \frac{L}{R} + O(1)}{2} \frac{\epsilon_2}{\epsilon_1} - \frac{2b^2}{L^2} zE \tag{30}$$

i.e.,

$$E = \frac{E^\infty \cos(\theta)}{1 + \left(\ln \frac{L}{R} + O(1) \right) \frac{\epsilon_2 b^2}{\epsilon_1 L^2}} \tag{31}$$

[Also can calculate $O(1)$ terms for ellipse and find $\ln \frac{L^2 - z^2}{R^2(z)} = \ln \frac{L^2}{b^2}$.]

The effective modulus for a composite/dispersion with number density n of inclusions (number of inclusions per unit volume), and arbitrary orientation ($\langle \cos\theta \rangle = 1/3$), is

$$\begin{aligned} \epsilon^* &= \epsilon_1 - \frac{n}{3} \int_{-L}^{L} z q(z) dz \\ &= \epsilon_1 \left[1 + nL^3 \frac{4\pi}{9} \frac{\epsilon_2 b^2}{\epsilon_1 L^2} \frac{E}{E^\infty} \right] \\ &= \epsilon_1 \left[1 + \frac{4\pi}{9} nL^3 \frac{\alpha^2}{\frac{\epsilon_1}{\epsilon_2} + \left(\ln \frac{1}{\alpha} + O(1) \right) \alpha^2} \right] \end{aligned} \tag{32}$$

where $\alpha \equiv \frac{b}{L} \approx \frac{R}{L}$ (the aspect ratio of the inclusion).